The Analysis of Multi-Year Low-Level and Mid-Level Mixed-Phase Clouds Observed at the North Slope of Alaska Cloud and Radiation Testbed Site

Z. Wang
University of Wyoming
Laramie, Wyoming

K. Sassen
University of Alaska
Fairbanks, Alaska

D. Whiteman and B. Demoz
NASA Goddard Space Flight Center
Greenbelt, Maryland

Introduction

The impact of a cloud system strongly depends on the cloud microphysical properties and its vertical extent (Stephens et al. 1990; Baker 1997). Although clouds can contain only water droplets when > 0°C and only ice crystals when < –40°C, between 0 and –40°C, clouds can be of ice, water, or mixed-phase composition (Rauber and Tokay 1991; Cober et al. 2001). Among them, mixed-phase clouds are poorly understood. However, properly representing them in general circulation models (GCMs) is very important for climate simulations (Fowler et al.1996; Li and Le Treut 1992; Sun and Shine 1994; Gregory and Morris 1996). The internal structures of mixed-phase clouds have large variations among different cloud types and latitudes. In low- and mid-latitude, mixed-phase clouds are often associated with convective clouds, on the other hand, mixed-phase clouds usually exist in stratiform in the Polar region.

The results of the Surface Heat Budget of the Arctic (SHEBA) experiment indicate that most of Arctic boundary layer clouds are mixed-phase clouds (Shupe et al. 2001; Intrieri et al. 2002). Therefore, mixed-phase clouds play a particularly important role in the Arctic climate system. Curry et al. (1996) gave a comprehensive review of arctic clouds and their role in the Arctic climate system, and clearly indicated that clouds are important to better understand arctic cloud-radiation-surface-dynamics feedbacks. The recent study of Vavrus (2004) indicated that cloud-feed back contribute significantly to the Arctic worming. To better predicate climate change in the Arctic, we need to better understand mixed-phase cloud and to improve it representation in GCMs.

Mixed-phase cloud microphysical properties have been mainly studied with in situ measurements (Fleishauer et al. 2002; Hogan et al. 2003; Korolev et al. 2003), which provide detailed microphysical properties to understand the physical processes controlling mixed-phase clouds. To better understand

mixed-phase clouds in different climate regions over a long period, we have to explore the capability of remote sensing. Radar-only based remote sensing algorithms of mixed-phase clouds (Sauvageot 1996; Vivekanandan et al. 1999; Shupe et al. 2004) are not practical for many stratiform mixed-phase clouds, especially in the Polar region. Based on The Department of Energy Atmospheric Radiation Measurement (ARM) program Cloud and Radiation Testbed sites observations, we developed a new algorithm to retrieve the microphysical properties of supercooled water with ice virga, a major type of mixed-phase cloud in the Arctic, by combining active and passive remote sensor measurements (Wang et al. 2004).

To better characterize arctic mixed-phase cloud, we are applying the algorithm to the longtime multi-sensor observations at the North Slope of Alaska (NSA) Cloud and Radiation Testbed site. This paper presents two case studies and initial statistical results of mixed-phase cloud microphysical and macrophysical properties observed at the NSA site.

Observations

The observations used in this study are from two active sensors: Millimeter-wavelength cloud radar (MMCR) and Micropulse lidar (MPL), and two passive sensors: Microwave radiometer (MWR) and atmospheric emitted radiance interferometer (AERI). The MMCR is a zenith-pointing radar with a 2-m diameter antenna that operates at 34.86 GHz (8.7-mm wavelength); it has a sensitivity of about -50 dBZ at 5.0 km altitude. This powerful Doppler radar, working in cycles of four sequential modes with selectable parameters, can detect most of the clouds in the troposphere from stratus to cirrus. The MPL is a compact eye-safe lidar that measures cloud base heights and aerosol profiles from the surface to about 20 km in the absence of strongly attenuating clouds. Eye-safety allows for full-time, long-term unattended operation, and is achieved by transmitting low power pulses through an expanded beam, with a much higher pulse repetition frequency than that used in standard lidar systems. The MMCR can penetrate optically thick clouds to detect multi-layer cloud systems. However, its long wavelength limits its capability to detect midlevel supercooled water clouds with relatively small water droplets. For mixed-phase clouds or water clouds with drizzle, MMCR signals are dominated by the backscatter of ice particles or drizzle-size droplets. MPL are sensitive enough to detect all clouds in the troposphere expect for optically thin cirrus during day time. The main limitation for MPL and other ground-based lidar is that the strong attenuation of clouds limits lidar capability to detect upper cloud layer in the presence of low-level optically thick cloud layer. Combining MMCR and MPL provide us better capability for cloud detection (Wang and Sassen 2001).

The MWR receives nadir microwave radiation from the sky at 23.8 GHz and 31.4 GHz. Path integrated water vapor and liquid water can be retrieved from MWR measurements. Statistical retrieval methods are usually employed to derive water vapor path and liquid water path (LWP) from the total absorption. In current ARM data, the regression residual error or 'theoretical accuracy' of LWP is about 0.03 mm (30 g/m^2) or 10 times the sensitivity or noise limit (0.003 mm) of the MWR. This detectable level limits MWR capability to measure the LWP of many supercooled clouds and mixed-phase clouds.

The "heart" of the AERI radiometer is a Fourier-transform infrared (IR) spectrometer, including the calibration blackbodies with temperature controllers. The AERI measures the absolute infrared spectral radiance of the sky also in the nadir direction. The spectral measurement range of the instrument is

500 to 3300 cm^{-1} (20 to 3 μm) with a spectral resolution of 1.0 cm^{-1}. In our algorithm, we use AERI measurements to retrieve water dominated source cloud property. Compared with the MWR, AERI based retrieval covers the low LWP case. Therefore, Combining MWR and AERI measurements, we are able to cover the full spectrum of LWP observed in the Arctic.

The NSA Cloud and Radiation Testbed site observations start from May 1998. But observations with all above instruments are not available until January 1999. We are analyzing observations from January 1999 to August of 2004.

Summary of the Algorithms

Cloud Phase Identification

The easiest way for cloud phase identification is to use lidar linear depolarization measurements (Sassen 1991). How the measurements is not available at the NSA Cloud and Radiation Testbed site until 2004. To use MPL measurements as early as 1998, we need an alternative way for cloud phase identification at the NSA Cloud and Radiation Testbed site. The microphysical property differences between water and ice clouds make it possible to use single lidar channel measurements to identify water layer. Figure 1 presents the distribution of clouds in terms of cloud extinction coefficient and linear depolarization ratio based on SHEBA depolarization lidar and MMCR measurements. Water and ice clouds are clearly grouped into two separated clusters in this 2D plot, which clearly indicates that cloud extinction coefficient provides cloud phase information as well as lidar linear depolarization ratio.

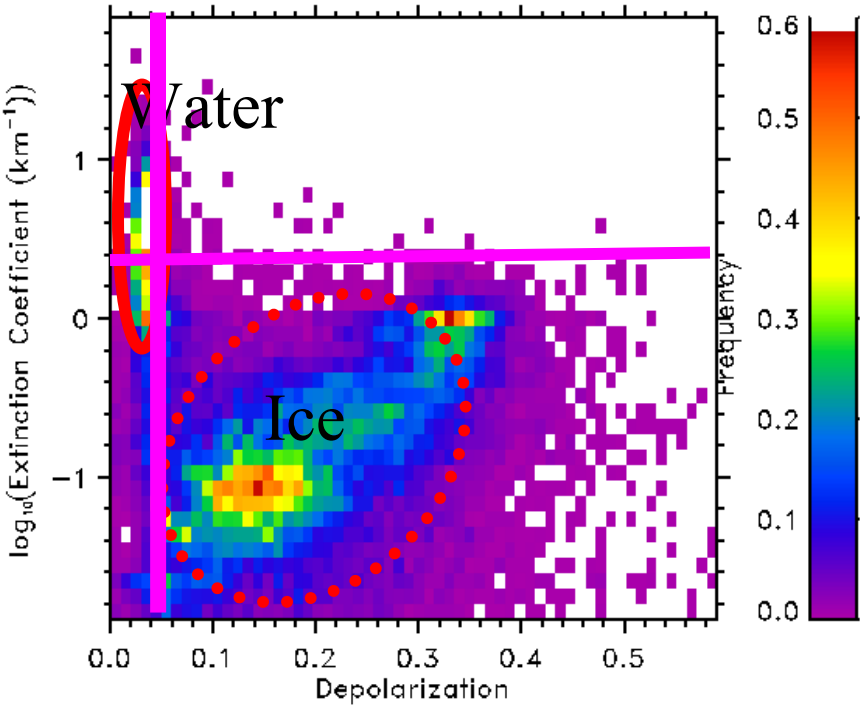

Figure 1. The frequency distribution of clouds in terms of lidar linear depolarization and extinction coefficient based on SHEBA data.

With results indicated in the above figure, we are able to identify cloud phase from single channel MPL measurements with the following steps:

Detect cloud and virga or precipitation bases from MPL return power (Wang and Sassen 2001).

1. Retrieval cloud extinction coefficient profile.
2. Combining maximum extinction coefficient and thickness to confirm water layer.
3. Combing temperature and virga and precipitation depth for ice identification.
4. A cloud layer include both water and ice is regarded as mixed-phase cloud

MMCR measurements may fail to detect supercooled water clouds, but are good at detecting ice particles. Therefore, combining MMCR with MPL measurements, we will be able to better identify mixed-phase clouds in the NSA site. The combined MMCR and MPL approach is underdevelopment and validation.

Mixed-phase Cloud Microphysical Property Retrieval

Supercooled water with ice virga can be generally regarded as two connected cloud layers where the top is the supercooled water-dominated source cloud and the bottom is an ice cloud, although it is also necessary to study ice within the water-dominated source cloud. First, we treat ice virga as an independent ice cloud, and apply an existing lidar-radar algorithm to retrieve ice water content (IWC) and general effective size (D_{ge}) profiles (Wang and Sassen 2002). Then a new iterative approach is used to retrieve supercooled water cloud properties (LWP and effective radius r_{eff}) by minimizing the difference between atmospheric emitted radiance interferometer (AERI) observed radiances and radiances calculated using the discrete ordinate radiative transfer model at 12 selected wavelengths. The flowchart of the algorithm is given in Figure 2, and more information about the algorithm can be found from Wang et al. (2004). Case studies demonstrated the capabilities of this approach in retrieving radiatively important microphysical properties to characterize this type of mixed-phase cloud. The good agreement between visible optical depths derived from lidar measurement and those estimated from retrieved liquid water path and effective radius provided a closure test for the accuracy of mainly AERI-based supercooled water cloud retrieval.

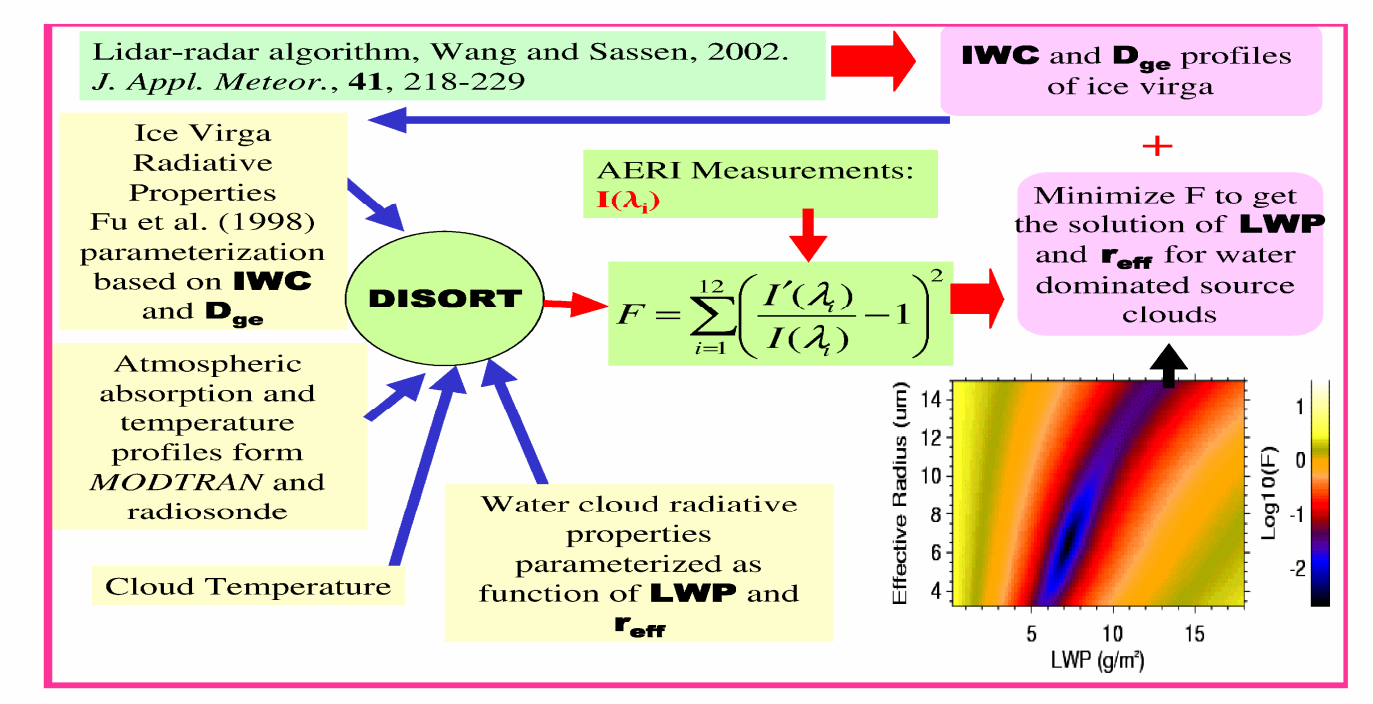

Figure 2. The flowchart of mixed-phase microphysical property retrieval algorithm

Case Studies

The algorithm is applied to the data from the NSA Cloud and Radiation Testbed site. To show the algorithm capability, we briefly discussed two cases in this section. The first case is a boundary-layer supercooled stratocumulus with ice precipitation. Figure 3 shows radiosonde temperature and relative humidity (RH) profiles obtained at the NSA site at 2259 UTC 1 November 2001. This cloud system lasted more than 30 hours, and the 24-hour observations of MMCR and MPL and retrieved ice and water properties are presented in Figure 4. The supercooled stratocumulus clouds are clearly indicated by narrow bright band in the time-height display of MPL extinction (Figure 4b). The ice precipitation is more clearly displayed by Z_e profiles in Figure 4a. The cloud top increased slowly from ~1.5 to ~2.4 km during the 24-hour period. Cloud top temperature was about -26°C at 2259 UTC, and there was ~4°C temperature inversion above the cloud top. The RH profile shows relative moisture environments above and below the supercooled water-dominated generating layer. This may be an important factor for the maintenance of this type mixed-phase clouds.

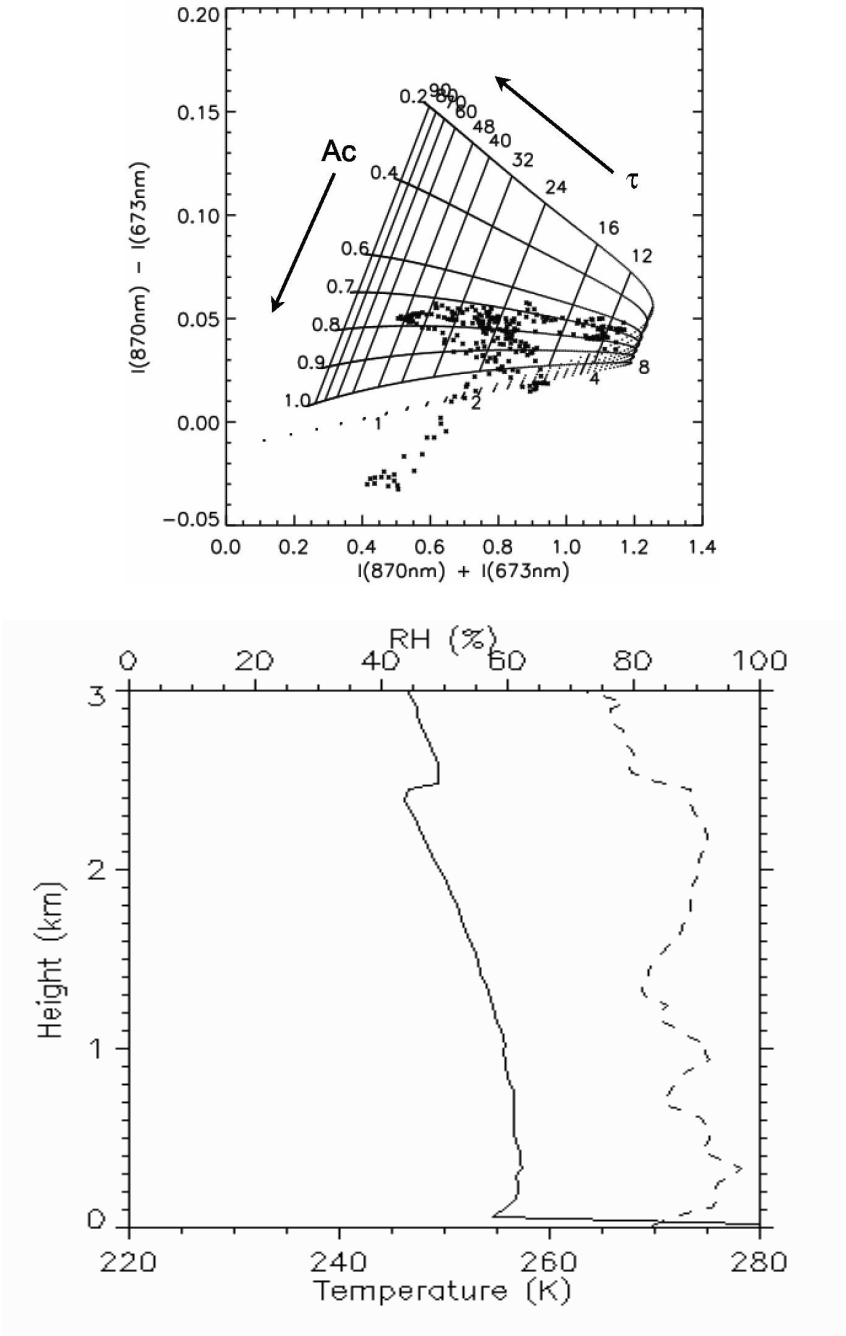

Figure 3. Radiosonde temperature (solid line) and relative humidity (dashed line) profiles obtained at the NSA site at 2259 UTC 1 November 2001.

The retrieved IWC and D_{ge} profiles of ice precipitation are given in Figure 4c and d. The IWC values range from a few mg/m^3 to ~ 100 mg/m^3, and are usually increase when height decrease because the boundary layer was ice saturated. The D_{ge} of ice precipitation were between 60 and 160 um. The LWP and reff of the supercooled water-dominated generating layer are given in the Figure 4e. The algorithm

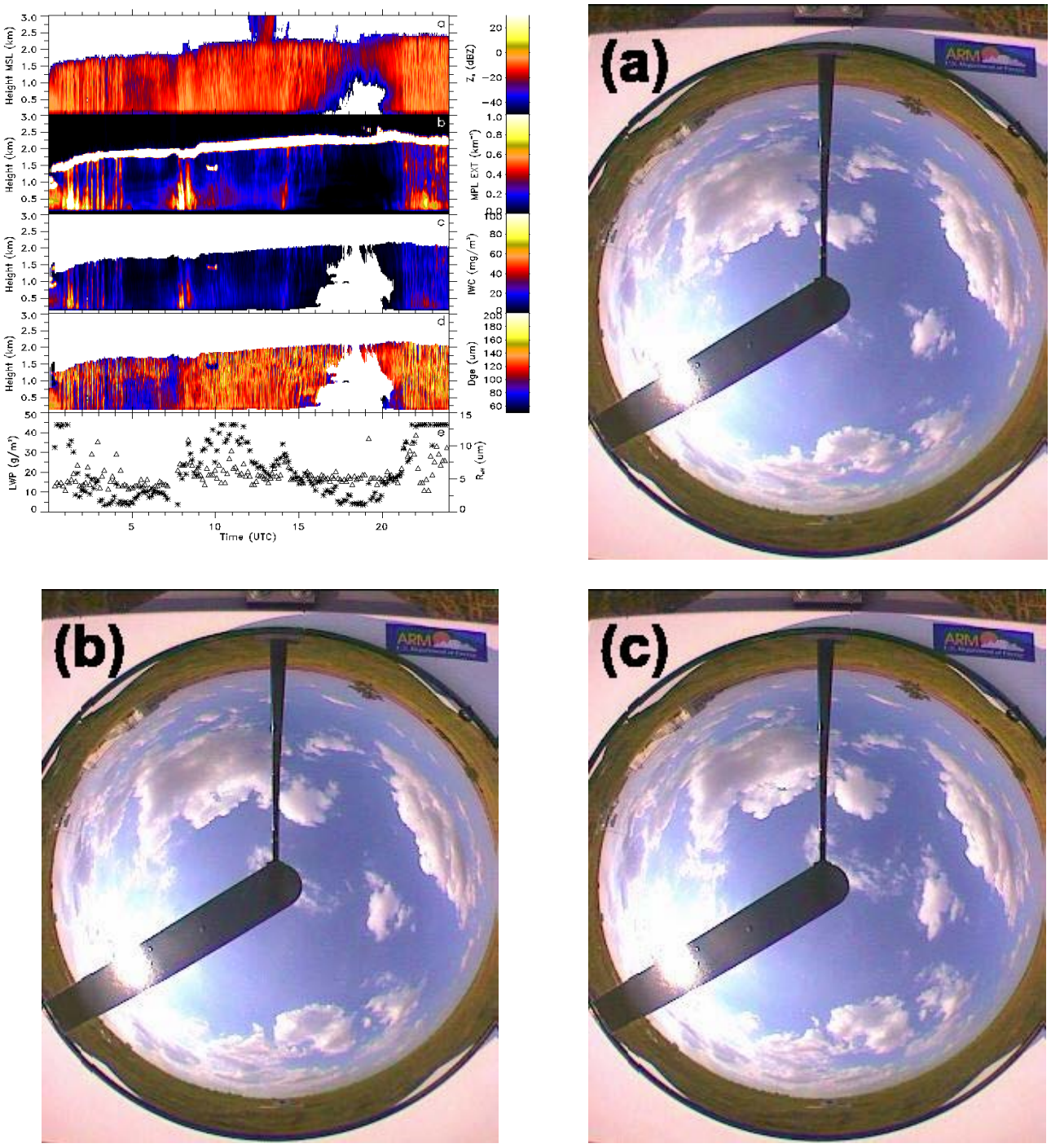

Figure 4. Time-height display of radar reflectivity factor (Z_e, a), visible extinction coefficient retrieved from MPL measurements (b), the retrieved IWC (c) and D_{ge} (d) profiles, and supercooled water cloud properties for a stratocumulus cloud with ice precipitation observed at the NSA Cloud and Radiation Testbed site on 1 November 2001.

only can be applied to water cloud with LWP smaller than some values depending somewhat on particle size (Wang et al. 2004). The largest LWP in the retrieval is set at 45 g/m^2, and we use MWR measurements when LWP is larger than this value. Figure 4e shows a large variation of LWP while r_{eff} values are mainly around 5 um.

The second case is an interesting altocumulus with ice virga observed at the NSA Cloud and Radiation Testbed site on 2 January 2002, which transited to all ice altostratus in a short period. Figure 5 shows radiosonde temperature and relative humidity (RH) profiles obtained at the NSA site at 2259 UTC 2 January 2002. The time-height displays of MMCR and MPL measurements and retrievals of cloud microphysical properties are presented in Figure 6a-e. The supercooled water existed until ~ 12 UTC at ~5.5 km height. There was no radiosonde data available during the supercooled water cloud occurrence; however, radiosonde data at 2259 UTC indicates -30°C at the supercooled water cloud height.

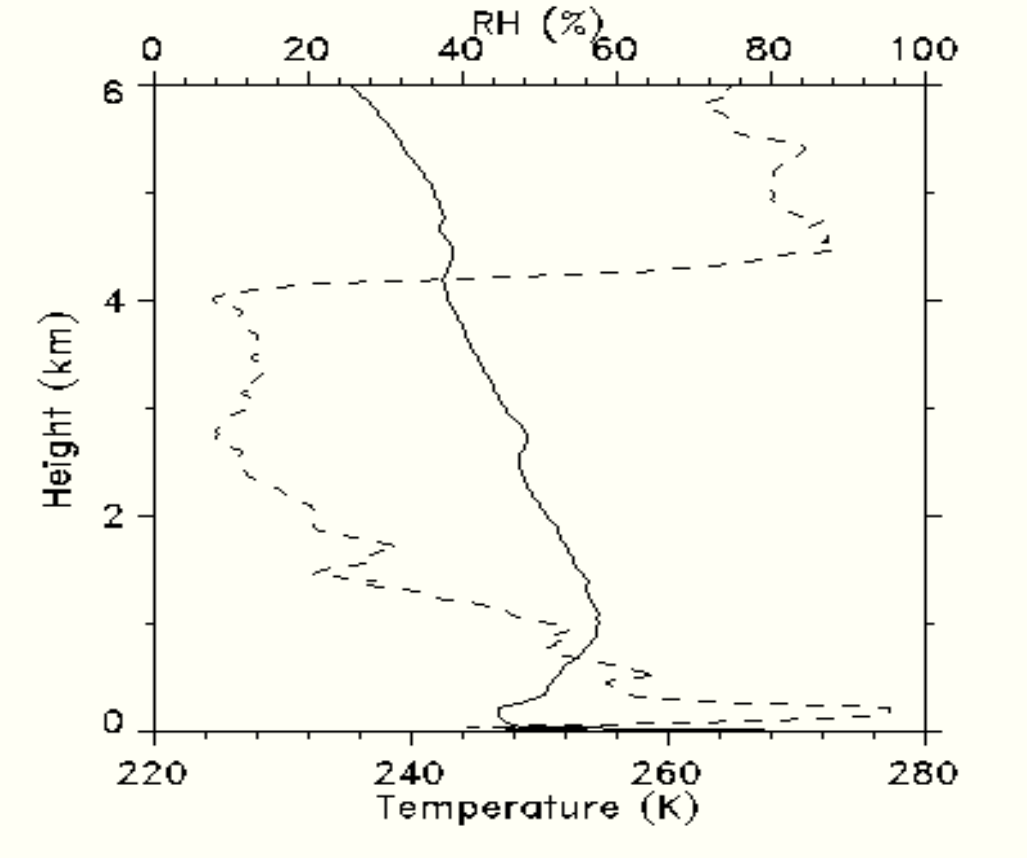

Figure 5. Radiosonde temperature (solid line) and relative humidity (dashed line) profiles obtained at the NSA site at 2259 UTC 2 January 2002.

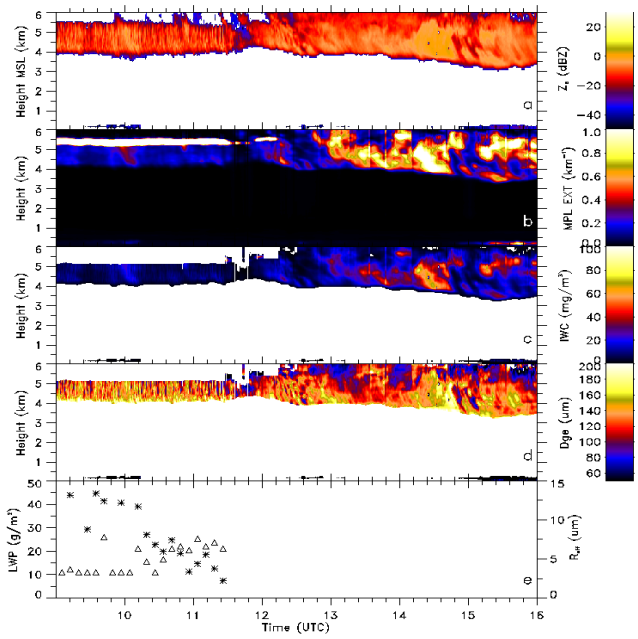

Figure 6. The same as Figure 4 except for an altocumulus with ice virga on 2 January 2002.

The transition of mixed-phase clouds to all ice clouds happened within an hour as indicated in Figure 6b. The IWC values of mixed-phase cloud are smaller than those during all ice period on average. However, the particle sizes of ice virga are similar to those at the same height during all ice period. This suggests that ice particle number concentration in the ice virga is smaller than that in all ice clouds. Understanding the factors maintaining the supercooled water clouds and controlling the transition in this case may be important to better understand cloud physics and dynamics in general, nevertheless, we lack the other necessary information to further explore it.

Cloud Macrophysical Properties Observed at the North Slope of Alaska Cloud and Radiation Testbed Site

A lidar cloud detection algorithm (Wang and Sassen 2001) is applied to MPL data observed at the NSA Cloud and Radiation Testbed site. The cloud phase identification is based on MPL measurements as discussed in Section 3.1. Figure 7 presents cloud occurrences of all clouds, ice clouds, and containing water (including water and mixed-phase clouds). The total cloud amount is compared with surface and satellite observations (Hahn et al. 1995, Schweiger et al. 1999). Although these data covered large area and averaged over long period, the NSA site observations show a good agreement with them. The data at the NSA Cloud and Radiation Testbed site also shows a large year to year variation of cloud cover (not showed here). Cloud layers contained water occurred only ~16% in March, but as high as ~80 % in August. A part of these clouds is mixed-phase clouds. Figure 7 clearly indicate that there is high occurrence of mixed-phase clouds during winter time. Because our cloud phase is based on MPL measurements, mixed-phase clouds with weak ice precipitation (weak lidar signal) do not classified as mixed-phase clouds in Figure 7. Therefore, the occurrence of mixed-phase clouds will be slightly higher if we include these cases. We are working to combine MPL and MMCR measurements to better identify mixed-phase clouds.

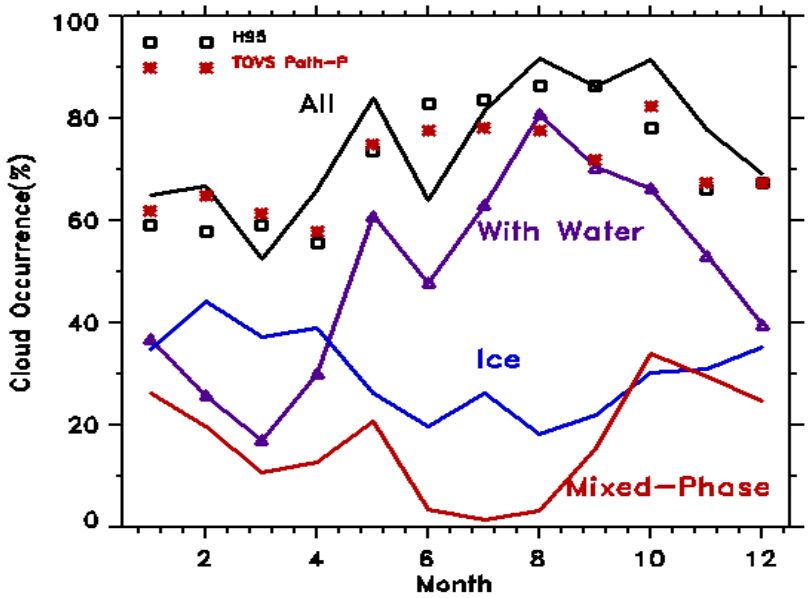

Figure 7. The occurrences of ice, mixed-phase, with water, and all type clouds based on the NSA MPL data. The category of with water includes water and mixed-phase clouds and fogs. The results indicate that it is very cloudy at the NSA site. The all cloud occurrence agrees well with other surface (H95, Hahn et al. 1995) and satellite (TOVA Path-P, Schweiger et al. 1999) measurement in the Arctic.

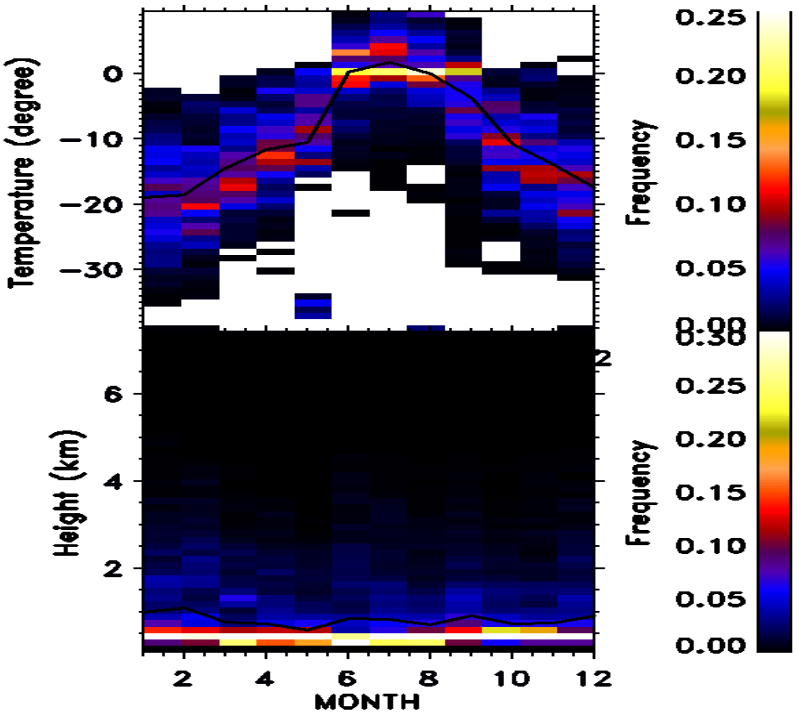

Figure 8. The distributions of cloud (containing water) base temperature and height observed at the NSA Cloud and Radiation Testbed site.

The frequency distributions of water layer base (including both mixed-phase and pure water clouds) temperature and height for each month are given the Figure 8. There is no surprise that there is a strong annual variation of the cloud base temperature. During January, the mean base temperature reaches ~ -19°C. Excluding June, July, August, and September, over 95% water layers are supercooled. The water base height mainly locates in the boundary layer. The mean base height ranges from ~500 m to ~1000 m.

The Statistical results of the microphysical properties of Arctic mixed-phase clouds

The statistical results of microphysical properties of arctic mixed-phase clouds based on ~150 different cases are presented in Figures 9 and 10. Figure 9 shows the frequency distributions of LWP, r_{eff}, and visible optical depths for ice and water. These results indicate a large variation of microphysical properties of this type of mixed-phase clouds. Compared with boundary-level pure water clouds, the LWP of mixed-phase clouds is smaller. The optical depth of ice virga is much smaller than that of water in this type of mixed-phase clouds in general, but it shows a large variation at different stages of cloud lifecycle as revealed in the case studies.

The statistical results of LWP retrieved from MWR measurements (clear sky biases are corrected) for same cases are presented in Figure 9 for comparison. Although, there is good overlap over 10-30 g/m^2 range between these two methods, the MWR retrieved LWP has a positive bias on average when LWP is below 30 g/m^2, especially, when clear sky biases are not corrected.

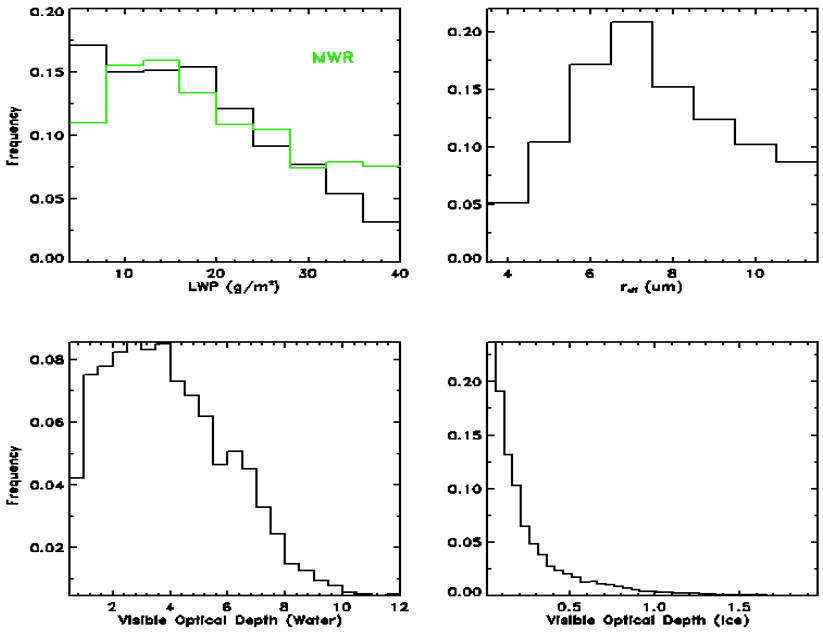

Figure 9. Frequency distributions of LWP, r_{eff}, and the optical depth of supercooled water and ice virga. The frequency distribution of LWP derived from MWR during the same period is plotted in green color.

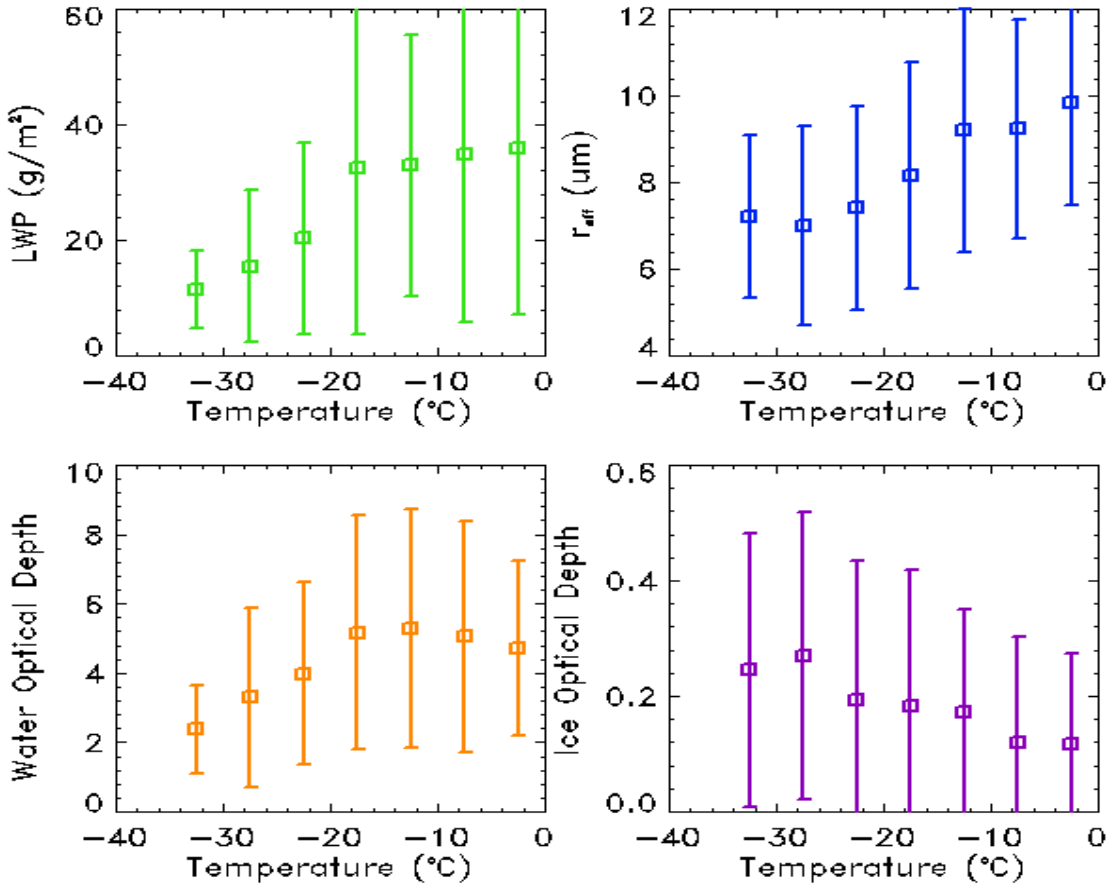

Figure 10. The temperature dependencies of LWP, r_{eff}, and water and ice optical depths. Vertical lines represent standard deviations.

The temperature dependencies of LWP, r_{eff}, and water and ice optical depths are presented in Figure 10. LWP and r_{eff} increase with the increase of cloud temperature. Water optical depth increases with cloud temperature increase until ~ -15° C then start decrease slightly. On the other hand, ice optical depth decrease with increase of cloud temperature. The different temperature dependencies of water and ice optical depths suggest that the contribution of ice in the total optical depth increase with decrease of cloud temperature. The standard deviations of them are given with vertical lines, which indicate large variations of mixed-phase cloud properties at given temperatures because many other parameters also control cloud microphysical properties. In the mixed-phase clouds as we studied here, the competition between ice and water phases makes the situation more complicated.

Summary

Based on MPL measurements, the cloud occurrence at the NSA Cloud and Radiation Testbed site is as high as 90% during the Arctic summer season. Except January to April, more than 50% of cloud layer include water layer. The statistical results of water layer base height and temperature indicate a high occurrence of supercooled water clouds in the Arctic. In the Arctic, the supercooled water layer usually

co-exists with an ice virga layer or ice precipitations to from a simple type mixed-phase cloud. A better characterization of this type mixed-phase cloud is important to better understand the role of clouds in the arctic climate system.

An approach of combining lidar, radar and radiometer measurements to retrieve the microphysical properties of this type mixed-phase clouds was developed. The approach can retrieve the microphysical properties of water and ice in the cloud layer, which are necessary to better understand cloud microphysical processes in this type of mixed-phase cloud. The retrieval accuracy of LWP and r_{eff} for water-dominated generating layer is ~15%.

The two case studies illustrated the capability of the algorithm for characterizing this type mixed-phase clouds. The initial statistics of microphysical properties of this type of mixed-phase clouds based on ~150 cases are presented. There are apparent temperature dependences for both LWP and reff of the water-dominated source clouds. The temperature dependencies of water and ice optical depths suggest that ice contribution in this type mixed-phase cloud increase with the decrease of cloud temperature. Comparison of the retrieved LWP with that retrieved from MWR indicated that MWR is unable to provide reliable low LWP measurements for supercooled altocumulus with ice virga. The bias of MWR retrieved LWP can up to 20 g/m^2 for a given case, which is significant in terms of resulting radiative impacts.

The results presented here are preliminary. The analysis of long-term NSA Cloud and Radiation Testbed site observations is still in progress. Combining retrieved microphysical properties with other observations and model simulations, we are aiming at better understanding the generation, maintenance, and impact of this type mixed-phase cloud in the Arctic.

Acknowledgements

This research has been funded by DOE Grant DE-FG02-03ER63536 and DE-FG03-03ER63530 from the Atmospheric Radiation Measurement program.

References

Baker, MB. 1997. "Cloud microphysics and climate." *Science* 276, 1072-1078.

Cober, SG, GA Isaac, AV Korolev, and JW Strapp. 2001. "Assessing cloud phase condition conditions." *Journal of Applied Meteorology* 40, 1967-1983.

Curry, JA, WB Rossow, D Randall, and JL Schramm. 1996. "Overview of Arctic cloud and radiation characteristics." *Journal of Climate* 9, 1731-1764.

Fleishauer, RP, VE Larson, and TH Vonder Haar. 2002. "Observed microphysical structure of midlevel, mixed-phase clouds." *Journal of Atmospheric Science* 59, 1779-1804.

Fowler, LD, DA Randall, and SA Rutledge. 1996. "Liquid and ice cloud microphysics in the CSU general circulation model. Part I: model description and simulated microphysical processes." *Journal of Climate* 9, 489-529.

Gregory, D and D Morris. 1996. "The sensitivity of climate simulation to the specification of mixed phase clouds." *Climate Dynamics* 12, 641-651.

Hahn, CJ, SG Warren, J London. 1995. "The Effect of Moonlight on Observation of Cloud Cover at Night, and Application to Cloud Climatology." *Journal of Climate* 8: 1429-1446.

Hogan, R, P Francis, H Flentje, AJ Illingworth, M Quate, and J Pelon. 2002. "Characteristics of mixed-phase clouds part I: lidar, radr and aircraft observations from CLARE'98." *Quarterly Journal of the Royal Meteorological Society* 129, 2089-2116.

Hogan, R, AJ Illingworth, EJ O'Connor, and JPVP Baptista. 2003. "Characteristics of mixed-phase clouds part I: A climatology from ground-based lidar." *Quarterly Journal of the Royal Meteorological Society* 129, 2117-2134.

Intrieri, JM, MD Shupe, T Uttal, and BJ McCarty. 2002. "An annual cycle of Arctic cloud characteristics observed by radar and lidar at SHEBA." *Journal of Geophysical Research* 107, 8030, doi:10.1029/2000JC000423.

Korolev, AV, GA Isaac, SG Cober, JW Strapp, and J Hallett. 2003. "Microphysical characterization of mixed-phased clouds." *Quarterly Journal of the Royal Meteorological Society* 129, 39-65.

Li, Z-X, and HL Treut. 1992. "Cloud-radiation feedbacks in a general circulation model and their dependence on cloud modeling assumptions." *Climate Dynamics* 7, 133-139

Rauber, RM, and A Tokay. 1991. "An explanation for the existence of supercooled water at the tops of cold clouds." *Journal of Atmospheric Science* 48, 1005-1023.

Sassen, K. 1991. "The polarization lidar technique for cloud research: A review and current assessment." *Bulletin of the American Meteorological Society* 72, 1848-1866.

Sauvageot, H. 1996. "Retrieval of vertical profiles of liquid water and ice content in mixed clouds from Doppler radar and microwave radiometer measurements." *Journal of Applied Meteorological* 35, 14-23.

Schweiger, AJ, RW Lindsay, JR Key, JA Francis. 1999. "Arctic clouds in multiyear satellite data sets." *Geophysical Research Letter* 26, 1845-1848.

Shupe, MD, T Uttal, SY Matrosov, AS Frisch. 2001. "Cloud water contents and hydrometer sizes during the FIRE-Arctic cloud experiment." *Journal of Geophysical Research* 106, 15,015-15,028.

Shupe, MD, JM Intrieri. 2003. "Cloud radiative forcing of the Arctic surface: The influence of cloud properties, surface albedo, and solar zenith angle." *Journal of Climate* 17, 616-628.

Stephens, GL, S Tsay, PW Stackhouse, and PJ Flatau. 1990. "The relevance of the microphysical and radiative properties of cirrus clouds to climate and climatic feedback." *Journal of Atmospheric Science* 47, 1742-1753.

Sun, Z, and KP Shine. 1994. "Studies of the radiative properties of ice and mixed-phase clouds." *Quarterly Journal of the Royal Meteorological Society* 120, 111-137.

Vavrus, S. 2004. "The impact of cloud feedbacks on Arctic climate under greenhouse forcing." *Journal of Climate* 17, 603-615.

Vivekanandan, J, BE Martner, MK Politovich, and G Zhang. 1999. "Retrieval of atmospheric liquid and ice characteristics using dual-wavelength radar observations." *IEEE Transactions of the Geosciences Remote Sensing* 37, 2325-2334.

Wang, Z and K Sassen. 2001. "Cloud type and macrophysical property retrieval using multiple remote sensors." *Journal of Applied Meteorology* 40, 1665-1682.

Wang, Z and K Sassen. 2002. "Cirrus cloud microphysical property retrieval using lidar and radar measurements: I algorithm description and comparison with in situ data." *Journal of Applied Meteorology* 41, 218-229.

Wang, Z, K Sassen, D Whiteman, and B Demoz. 2004. "Studying altocumulus plus virga with ground-based active and passive remote sensors." *Journal of Applied Meteorology* 43, 449-460.